References and Notes

(1) Iannelli, P.; Immirzi, A. *Macromolecules*, preceding paper in this issue.
(2) Immirzi, A.; Iannelli, P. *Gazz. Chim. Ital.* **1987**, *117*, 201.
(3) Immirzi, A.; Iannelli, P. *Macromolecules* **1988**, *21*, 768.
(4) Arnott, S.; Wonacott, A. J. *Polymer* **1966**, *7*, 157.
(5) Tanaka, T.; Chatani, Y.; Tadokoro, H. *J. Polym. Sci., Polym. Phys. Ed.* **1974**, *12*, 112.
(6) Tadokoro, H. *Structure of Crystalline Polymers*; Wiley: New York, 1979.
(7) Benedetti, E.; Pedone, C.; Allegra, G. *Macromolecules* **1970**, *3*, 16.
(8) Johnson, C. K. In *Crystallographic Computing*; Ahmed, F. H., Ed.; Munksgaard: Copenhagen, 1970, pp 220–226.
(9) Allegra, G.; Benedetti, E.; Pedone, C. *Macromolecules* **1970**, *3*, 727.
(10) Cooper, M. J. *Acta Crystallogr., Sect. A: Found. Crystallogr.* **1982**, *A38*, 264.
(11) Cooper, M. S.; Rouse, K. D.; Sakata, M. *Z. Kristallogr.* **1981**, *157*, 101.

Structural Studies of Polymers with Hydrophilic Spacer Groups: Infrared Spectroscopy of Langmuir–Blodgett Multilayers of Preformed Polymers with Hydrocarbon Side Chains

J. Schneider and H. Ringsdorf

University of Mainz, D-6500 Mainz, FRG

J. F. Rabolt*

IBM Research Division, Almaden Research Center, 650 Harry Road,
San Jose, California 95120-6099.

Received March 21, 1988

ABSTRACT: A series of preformed polymers containing amphiphilic side chains and hydrophilic spacer groups in the backbone have been investigated by grazing incidence reflection and transmission infrared spectroscopy. In the former the electric field vector is normal to the film surface whereas in the latter, it is parallel to the surface. The two measurements taken collectively have provided information about the orientation of the ordered amphiphilic side groups and the partially disordered polymer backbone. The results indicate that there is a definite preferred orientation of the side chain axis normal to the substrate surface. The extent of this side chain order is affected by both the concentration of backbone spacer groups and the temperature of the Langmuir–Blodgett (LB) layers. These effects on the long-term aging of these polymeric multilayers will be discussed.

Introduction

It has long been recognized that thin films formed by Langmuir–Blodgett (LB) deposition offer an enticing alternative to films formed by conventional processing techniques.[1,2] In addition to being exceptionally thin (~25 Å) due to their molecular length, LB films can be molecularly designed so as to include functional chromophores within the individual layers.[3] Initially, many IR studies of LB multilayers[4–7] were focused on the assembly of fatty acid molecules on the water surface since closely packed stable structures could be formed and subsequently transferred to solid substrates. These investigations concentrated on determining order and orientation of cadmium arachidate,[6,7] $[C_{19}H_{39}COO^-]_2Cd^{2+}$, monolayers and multilayers transferred to reflective and transmissive substrates. Although this fatty acid was ideally suited for structural studies because of its high degree of order, it has been known for some time that multilayers do not have mechanical integrity and when submitted to aggressive environments (e.g., temperature and moisture), they undergo irreversible degradation.[8,9]

An attractive alternative was to incorporate within the amphiphilic molecules, reactive groups which could be polymerized by UV irradiation either on the water surface or on a solid substrate[10–13] in order to stabilize the films and provide mechanical strength. Unfortunately, contraction due to polymerization can lead to the creation of cracks and fissures[14–17] in the film, a trait undesirable especially if these films were to act as a diffusion barrier or insulating layer. In order to avoid this complication, recent interest has turned to the study of LB films of preformed polymers.[17] Initially, preformed homopolymers were investigated in order to assess the extent of molecular orientation and order. Tredgold and Winter[18] were the first to describe the deposition of LB monolayers of copolymers which first had to be hydrolyzed on the surface of the water subphase before transfer.

Recently, single monolayers of poly(octadecylmethacrylate) and poly(octadecylacrylate) (see Figure 1) were characterized by IR spectroscopy.[19] Dichroic studies indicated a preferential orientation of the *n*-alkyl side chains toward the surface normal with a loose intermolecular packing in the lattice. One possible reason for this lack of high orientation and order of the side chains can be attributed to their reduced mobility due to the stiffness of the polymer backbone. This particular problem has been addressed by Elbert et al.[17] with the incorporation of hydrophilic spacer groups into preformed polymers in order to increase the mobility of the monolayer. As a result, this reduced viscosity of the film promotes better self-organization of the amphiphilic side chains, therefore enhancing deposition behavior and multilayer quality.

It is the purpose of this work to report an IR study of a homopolymer and a series of related copolymers which contain amphiphilic side chains and various amounts of hydrophilic spacer group in the backbone[20] (see Figure 1). IR dichroic measurements have been made and utilized to determine the orientation of molecular groups in both the crystalline and amorphous components of the LB monolayers. The net result of incorporating hydrophilic spacer groups into the backbone on the molecular flexibility was investigated at room and elevated temperatures. This provided an assessment of the physical aging behavior[9] of these LB films which could then be compared

0024-9297/89/2222-0205$01.50/0

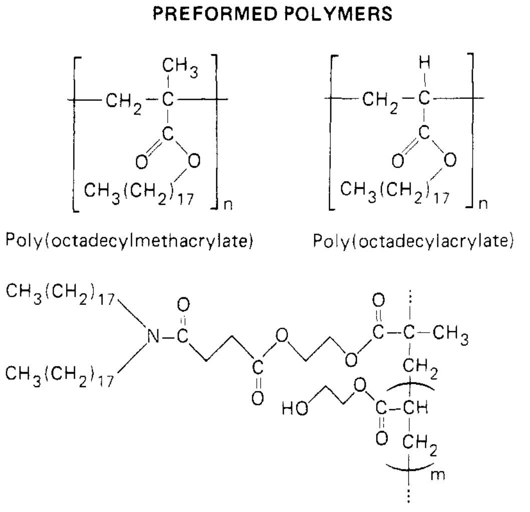

Figure 1. Chemical structures of preformed polymers studied by polarized infrared spectrocopy. Lower structure represents homopolymer ($m = 0$) and copolymers ($m = 1, 5, 10$) used in this study.

with similar results obtained for long chain fatty acid monolayers. In addition, a comparison of the IR results on the homopolymer and copolymers will be made with variable-temperature small-angle X-ray scattering (SAXS) studies of multilayered structures previously recorded.[21,22]

Experimental Section

The homopolymer and the copolymers $m = 1, 5$, and 10 were synthesized according to published procedures.[20] Gel permeation chromatography showed that the polymers prepared by radical polymerization are high molecular weight polymers with an average molecular weight of $\bar{M}_w = 7 \times 10^4$. Microanalysis was used to determine the statistical copolymer compositions.

The polymers were spread from chloroform solutions having a concentration of 0.5 mg/mL. A small amount of methanol was added to enhance solubility. The Langmuir–Blodgett multilayers were prepared on a commercially available film balance (Joyce Loebl) modified to include a Teflon tank. The water in the subphase was purified by deionization and passed through a Barnstead nanopure filtration system. The surface pressure of the monolayers was monitored by a Wilhelmy pressure pick up system. The monolayers (see Figure 2) of the preformed polymers were transferred at 20 °C as Y-type film (head-to-head, tail-to-tail).[23] Either zinc selenide disks (1-in. diameter) or 200 nm of silver evaporated onto microscope slides (1 in. × 3 in.) were used as substrates.

The zinc selenide disks were cleaned with a chloroform/methanol mixture (1/1), then treated by water spray, deionization bath, and 2-propanol water exchanger, and then finally dried at 100 °C. The microscope slides were first cleaned in an oxidative acid solution and then passed through the same cleaning procedure described above. The silver substrates were coated directly after evaporation of the metal films.

The surface pressure area diagrams (isotherms) of the polymers have been reported previously.[21,24] The surface pressure used for deposition was increased from 25 mN/m for the homopolymer to 30 mN/m for the copolymer $m = 1$, to 45 mN/m for $m = 5$, and to 50 mN/m for $m = 10$. Surface pressures during the deposition process were chosen accordingly to guarantee transfer of the condensed phase of the polymeric monolayers and to ensure monolayer stability. A dipping speed of 0.25 cm/min was chosen for all of the polymers. Drying periods of 20 min between subsequent dips are necessary to prevent retransfer of the previously deposited monolayer during the next dip downward, which was most notable for the copolymers with higher hydrophilic comonomer contents.

All infrared measurements were made with an evacuated IBM IR 98 FTIR interferometer. The spectra were recorded at 4 cm^{-1} resolution with a room-temperature deuteriated triglycine sulfate (DTGS) detector. To obtain spectra with high signal-to-noise ratios 2000 (or 4000) scans had to be collected.

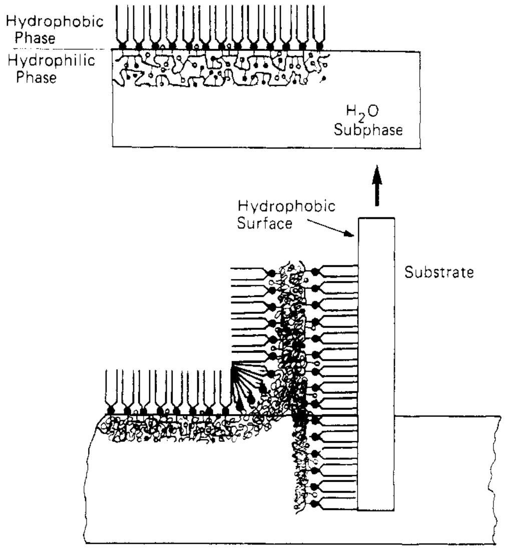

Figure 2. Schematic diagram of LB trough and multilayered deposition on a hydrophobic substrate.

For comparison the isotropic spectra of the polymers were taken by casting the bulk material from chloroform solutions onto KBr disks (1-in. diameter). The grazing incidence reflection spectra (electric field vector is perpendicular to the surface, $E_\perp$) were taken[25,26] from 12 layers on silver substrates. A standard Harrick Scientific reflection accessory with adjustable grazing angle between 80° and 88°[7] was used in conjunction with a heating device[27] to study the temperature induced molecular reorganization of these organic films. Only those groups which have a component of their change in dipole moment oriented perpendicular to the film would be observed.

The transmission spectra (electric field vector is parallel to the surface, $E_\parallel$) were obtained from six LB layers deposited on each side of a zinc selenide disk.

Results and Discussion

A. Transmission Measurements of Bulk Homopolymer and Copolymers. Shown in Figure 3 are the room temperature IR transmission spectra of the homopolymer ($m = 0$) and a series of copolymers ($m = 1, 5, 10$) with different amounts of hydrophilic spacer groups in the backbone. A close comparison reveals the presence of certain bands whose intensity is observed to change with increasing concentration of the hydrophilic spacer group. The two bands in the 1600–1800 cm^{-1} region are attributable to C=O stretching vibrations, with that at 1740 cm^{-1} resulting from the C=O stretch of the ester groups while the other at 1645 cm^{-1} originates from a vibration of the C=O bond of the amide group (see Figure 1). With the addition of ester groups in the hydrophilic main chain spacer, the 1740 cm^{-1} band intensity is observed to increase, such that in the $m = 10$ copolymer it is approximately three times the size of the same band in the homopolymer. Additional changes are observed in the 1000–1500 cm^{-1} region due to the increased spacer length. The CH_2 bending vibration ($\delta(CH_2)$) located at 1470 cm^{-1} and the 1380 cm^{-1} CH_2 wagging ($w(CH_2)$) band both appear as singlets in the homopolymer but gradually evolve into doublets with increasing comonomer concentration. Thus the shoulders observed at 1450 and 1400 cm^{-1} in the $m = 10$ copolymer can be attributed to vibrations of the CH_2 group in the backbone spacer (see Figure 1).

Also observed in this region are several broad bands which also show an interesting change in shape with increasing comonomer concentration. The band at 1260 cm^{-1} is very broad (80–100 cm^{-1}) and most likely due to a combination of CH_2 twisting and wagging vibrations in the main chain spacer. Thus its intensity would be expected

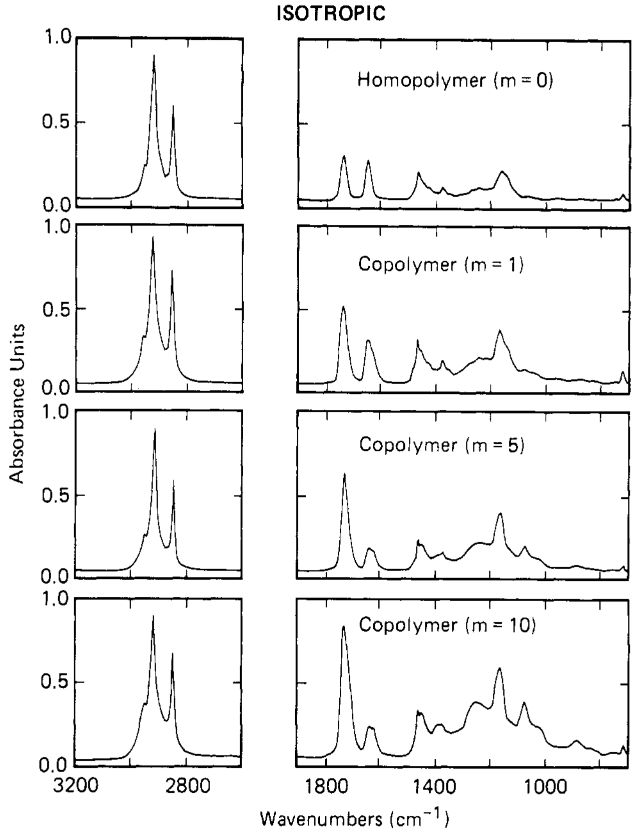

Figure 3. IR transmission spectra of solvent cast films of homopolymer (m = 0) and copolymers (m = 1, 5, 10) on KBr (resolution = 4 cm^{-1}; 250 scans).

to increase with m as is observed. Adjacent to this band is a strong doublet found at 1150 and 1170 cm^{-1} in the homopolymer. Interestingly enough the 1170 cm^{-1} component increases with an increased length of main chain spacer while the 1150 cm^{-1} component appears to be constant. Since both bands result from stretching vibrations of the C–O–C bonds of the ester groups, this would suggest that the 1150 cm^{-1} band is due to the motion of the ester group at the center of the side chain spacer while that at 1170 cm^{-1} can be attributed to a vibration of the COC groups adjacent to the polymer backbone. This would then account for its increase in intensity with increasing comonomer concentration.

As shown in the lower part of Figure 3, a band found at 1080 cm^{-1} with a broad shoulder at 1040 cm^{-1} is observed in the spectra of the copolymers but not in the homopolymer. Hence, its origin is obviously in the main chain spacer group. From a comparison with the spectrum of the homopolymer of the main chain spacer poly(2-hydroxy-ethylacrylate) (PHEA) not shown here, it is apparent that this medium intensity band is due to a stretching of the CO bond and a bending of the COH groups in the primary alcohol moiety. A weak band is present at 890 cm^{-1} in the PHEA spectrum and in the m = 5 and m = 10 copolymers of Figure 3, but its origin is as yet unclear.

Finally, all spectra in Figure 3 show the presence of a single band at 725 cm^{-1} attributable to a rocking vibration of the CH_2 group ($r(CH_2)$). The fact that these bands are all singlets indicates that the alkyl side chains do not pack in the orthorhombic unit cell found for LB films and bulk cadmium arachidate.[7]

A list of all these band assignments is included in Table I.

B. Polarized IR Spectra of Langmuir–Blodgett Multilayers. In order to assess the extent of orientation of individual segments of the polymer backbone and side chain, IR dichroic measurements of LB multilayers were undertaken. To obtain information about groups which have a component of the change in dipole moment perpendicular to the substrate, GIR measurements were made on Ag substrates. As Greenler[25] pointed out, this particular sampling geometry, with incident IR beam reflected at angles of 80–88° relative to the surface normal, results in an electric field component only perpendicular to the surface. On the other hand, in standard transmission measurements on ZnSe at normal incidence, the electric field vector is parallel to the surface. The combination of these two experiments provides information on the orientation of various parts of the polymer.

Table I
IR Band Assignments

frequency (cm^{-1})		
homopolymer[b]	copolymer (m = 10)[b]	assignmts[a]
2960 m	2960 m	$\nu_a(CH_3)$
2920 vs	2920 vs	$\nu_a(CH_2)$
2855 vs	2855 vs	$\nu_s(CH_2)$
1740 s	1740 vs	ν(C=O) ester
1645 s	1645 s	ν(C=O) amide
1470 s	1470 s, 1450 sh	$\delta(CH_2)$
1380 m	1400, 1380 m	$w(CH_2)$
1250 m br	1260 s br	$w(CH_2) + t(CH_2)$
1170, 1150 s	1170 s	ν(C-O-C)
1070 w	1080 s, 1040 sh	ν(C-O-H)
	890 m	
725 m	725 m	$r(CH_2)$

[a] Abbreviations: ν_a, asymmetric stretch; ν_s, symmetric stretch; δ, scissors; w, wag; r, rock. [b] Abbreviations: m, medium; s, strong; vs, very strong; w, weak; br, broad; sh, shoulder.

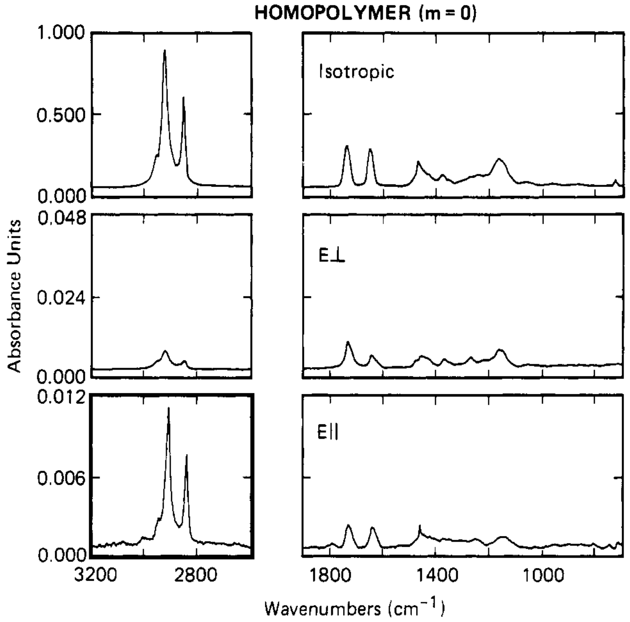

Figure 4. Comparison of grazing incidence reflection IR ($E_\perp$) and standard transmission ($E_\parallel$) measurements of homopolymer (m = 0). Spectrum of isotropic sample included for ease in comparison (resolution = 4 cm^{-1}; 4000 scans $E_\perp$, 2000 scans $E_\parallel$).

Shown in Figures 4 and 5 are the reflection and transmission spectra of the homopolymer and the m = 10 copolymer, respectively. Of particular interest is the CH_2 stretching region (3200–2600 cm^{-1}) where a dramatic change is observed in comparing $E_\parallel$ and $E_\perp$. In the former, the asymmetric CH_2 stretching vibration ($\nu_a(CH_2)$) at 2920 cm^{-1} and its symmetric ($\nu_s(CH_2)$) counterpart at 2855 cm^{-1} are seen to be much greater in intensity than the $\nu_a(CH_3)$ at 2960 cm^{-1} and the $\nu_s(CH_3)$ at 2870 cm^{-1}. This implies

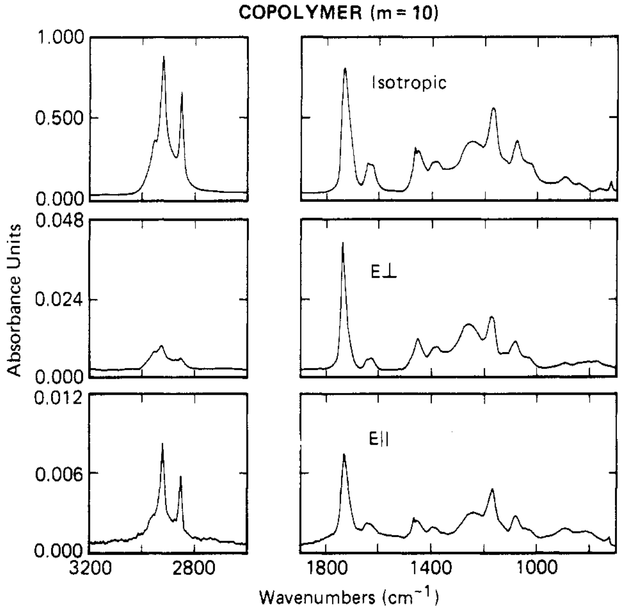

Figure 5. Comparison of grazing incidence reflection IR ($E_\perp$) and standard transmission ($E_\parallel$) measurements of copolymer (m = 10). Spectrum of isotropic samples included for ease in comparison (resolution = 4 cm^{-1}; 4000 scans $E_\perp$, 2000 scans $E_\perp$.) The overall intensity of the $E_\parallel$ spectrum appears to be weaker than that of the homopolymer even though there are 10 more spacer groups. This may be due to a transferability problem from the trough. Numerous repetitions did indicate that the relative intensities in the $E_\parallel$ spectrum are preserved.

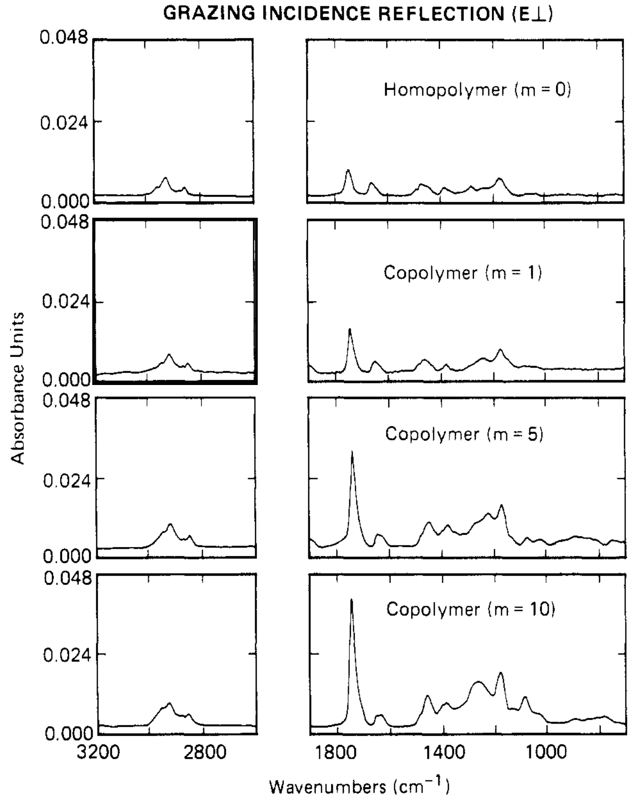

Figure 6. Comparison of $E_\perp$ spectra for homopolymer (m = 0) and copolymers (m = 1, 5, 10) (resolution = 4 cm^{-1}; 4000 scans).

that the plane of the CH_2 group is almost parallel to the substrate surface in the case of the m = 10 copolymer. Further support for this conclusion comes from the $E_\perp$ spectrum (shown in Figure 4) where the CH_2 stretches are more similar in intensity to the CH_3 stretching bands. In the ideal case of perfect orientation of the CH_2 planes parallel to the surface, the intensity of the CH_2 stretching band in $E_\perp$ would vanish. Although this is not the case in the homopolymer, there appears to be better orientation of the CH_2 planes parallel to the surface in the case of the copolymer (m = 10) as seen in Figure 5. In fact there is consistently a better organization of CH_2 planes parallel to the surface in proceeding from the homopolymer through the various copolymers (m = 1, m = 5, m = 10) indicating that the addition of main chain spacer units improves the orientation of the alkyl side chains perpendicular to the surface (see Figure 6). One possible explanation is that the increase in concentration of main chain spacer improves the self organization on the water surface prior to deposition due to an increase in the main chain flexibility. This would then allow a more efficient packing of the alkyl tails into two-dimensional crystals.

It should be pointed out that the addition of main chain spacer will also contribute intensity to this CH stretching region in the copolymer due to the addition of unordered CH_2 groups. However, their contribution will be to a broad background which will underlie the sharp CH_2 and CH_3 stretching vibrations of the ordered alkyl tails. This can be seen by comparison of Figures 4, 5, and 6.

The region between 1800 and 700 cm^{-1} also shows considerable dichroic effects indicating that parts of the main chain and side chain spacer may also be partially oriented. In the C=O stretching region, bands attributable to the ν(C=O) of the ester groups (1740 cm^{-1}) and of the amide group (1645 cm^{-1}) are found. In the homopolymer, these bands are comparable in intensity in $E_\parallel$ while in $E_\perp$ the ester C=O stretch is more intense than the amide C=O stretch. In the isotropic case these bands are observed to be comparable in intensity. This then suggests that the lack of intensity of amide C=O in $E_\perp$ is due to the fact that the amide C=O bond is inclined more parallel to the surface than perpendicular. This could be due to the geometric constraints around the amide nitrogen imposed by the alkyl tails. A similar obervation can be made for the m = 10 copolymer in Figure 5, although in this case the amide C=O appears to be a doublet. Since the addition of hydrophilic comonomer does not add any additional amide C=O groups, one possible origin of the low-frequency component at 1630 cm^{-1} is that it is due to H_2O molecules hydrogen bonded to this main chain spacer (see Figure 1).

In the 1500–1300 cm^{-1} region of the homopolymer are found the $\delta(CH_2)$ at 1470 cm^{-1} and the $w(CH_2)$ at 1380 cm^{-1}. The $\delta(CH_2)$ is very sharp and is observed only in $E_\parallel$ consistent with the model proposed earlier in which the alkyl tails are almost perpendicular to the substrate. There appears to be a second broad component underlying this sharp band and is due to the noncrystallizable CH_2 groups of the main-chain and side-chain spacer. Likewise disordered CH_2 groups are the origin of the broad 1380 cm^{-1} $w(CH_2)$ band since in crystalline n-paraffins no IR-active band is found at this position. Due to symmetry considerations only a weak Raman active vibration is observed in crystalline n-paraffins.

In the m = 10 copolymer (Figure 5), the broad shoulder at 1450 cm^{-1} has increased in intensity due to the addition of more CH_2 groups which are not in a crystalline environment. In addition a second component of the $w(CH_2)$ is observed at 1400 cm^{-1} which is due to the addition of main chain spacer CH_2 groups.

An additional multicomponent band associated with disordered CH_2 sequences is found in the 1200–1300 cm^{-1} region. As shown in the sequence of homopolymer and copolymer spectra of Figure 6 ($E_\perp$), it is obvious that this complex band contains at least two components at 1280 and 1235 cm^{-1}. These bands, also found in poly(ethyl-

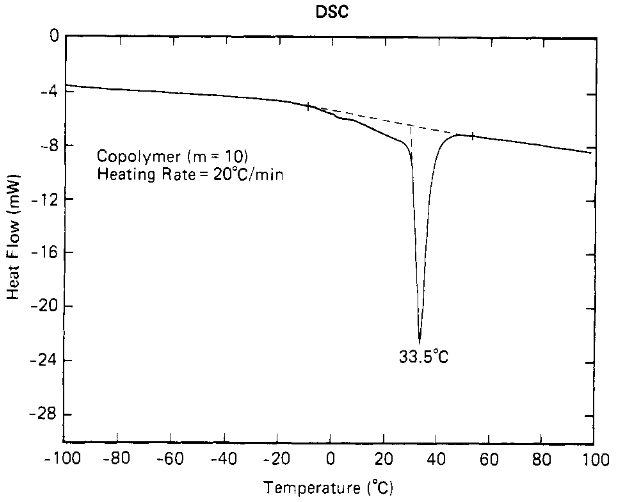

Figure 7. Differential scanning calorimetric trace of bulk sample of copolymer (m = 10) (heating rate = 20 °C/min; first heating).

eneoxide) (PEO),[28] aliphatic polyesters and poly(vinylacetate) (PVAc), can be attributed to a combination of CH_2 twist and wag vibrations. The large intensity changes observed in Figure 6 in this region upon the addition of CH_2 groups in the main chain spacer are consistent with this interpretation.

The remaining bands in the 1000–1200 cm^{-1} region involves the vibration of the C–O bonds of spacer groups. As described previously, the band at 1170 cm^{-1} contains a weaker shoulder at 1150 cm^{-1} which has been attributed to ν(C–O) of the ester group at the center of the side chain spacer. As shown in the spectra of the m = 10 copolymer of Figure 5, the most intense band is the 1170 cm^{-1} component, and compared to the intensity of the CH_2 twist and wag vibration at 1280 cm^{-1}, it is definitely more intense in the $E_\parallel$ spectrum. This would indicate that the plane of the C–O–C group in the main-chain spacer is preferentially oriented parallel to the surface. This is understandable due to the hydrophilic nature of the ester group.

The remaining strong band at 1080 cm^{-1} with a shoulder at 1040 cm^{-1} is absent in the homopolymer but is observed at high concentration of the main-chain spacer (m = 5, 10) as shown in Figure 6. Due to its presence in the IR spectra of the PHEA homopolymer, it is assigned to a stretching vibration of the terminal C–O–H group. It is also more intense (compared to 1280 cm^{-1} band) in the $E_\parallel$ spectrum of Figure 5 and also indicates that the plane of this group lies preferentially parallel to the surface.

Finally a weak band which consistently shows up only in $E_\parallel$ of the homopolymer and all copolymers at 725 cm^{-1} is due to the CH_2 rocking vibration of the alkyl side chains and further reaffirms that they are oriented with the CH_2 planes parallel to the surface.

C. Grazing Incidence Reflection IR Spectra of Copolymer (m = 10) at Elevated Temperature. Since it had been concluded in an earlier section that the alkyl side chains of the m = 10 copolymer exhibited the highest degree of orientation due to the flexibility of main chain produced by the incorporation of the highest concentration of spacer groups, this copolymer was investigated at elevated temperatures. In order to assess the extent of disorder introduced at high temperatures, only the CH_2 stretching region was monitored since differential scanning calorimetric (DSC) measurements (shown in Figure 7) indicated that a strong melting transition occurred at 33.5 °C and was associated with a disordering of the alkyl side chains. As shown in Figure 8, heating of this copolymer up above the bulk melting point causes a significant change in the ratio of the 2920 cm^{-1} $\nu_a(CH_2)$ and the 2855 cm^{-1} $\nu_s(CH_2)$ relative to the $\nu_a(CH_3)$ at 2960 cm^{-1}. Interestingly enough, cooling back to 22 °C results in a significant recovery of the initial order and orientation, although a complete return to the original intensities is not observed. As is shown in Figure 8, cycling to even higher temperatures does consistently disorder the alkyl side chains but cooling restores much of the order and orientation. Even at the temperature of 140 °C, a high degree of orientation returns after remaining at 22 °C for up to 1 week.

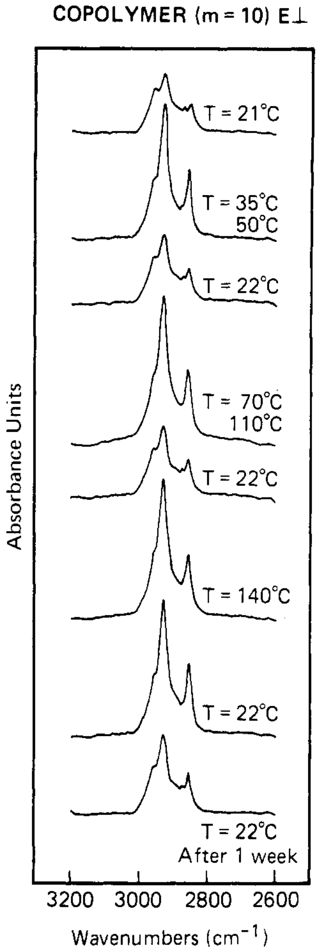

Figure 8. Comparison of IR spectra of CH_2 stretching region of copolymer (m = 10) as a function of temperature (resolution = 4 cm^{-1}; 4000 scans).

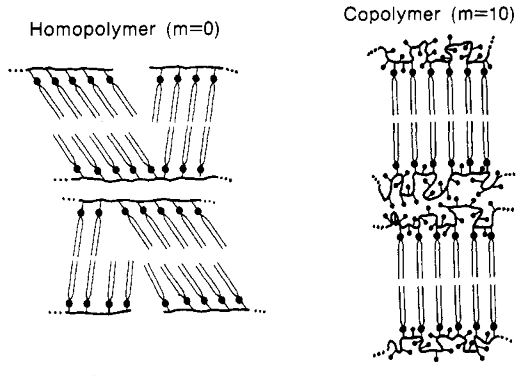

Figure 9. Model of the orientation of alkyl side chains in bilayer of homopolymer (m = 0) and copolymer (m = 10).

This exceptional thermal stability was also observed in a series of SAXS measurements of multilayers of this copolymer.[29] The SAXS intensity maximum observed at room temperature corresponds to the long period (in this case of a bilayer) of the layered structure and was the most intense for the m = 10 copolymer. This may be attributed to a higher degree of order found in this copolymer due to the increased flexibility of the main chain (Figure 9). Our infrared studies support this explanation.

Upon heating LB multilayers of the homopolymer and copolymers, it was found that the $m = 10$ copolymer could be heated beyond 160 °C before its SAXS maximum disappeared. At temperatures of 160 °C, the SAXS maximum is still present but weaker than that found at room temperature.[29] Similar observations have been made previously[21] for a series of copolymers containing acrylic acid comonomers.

It is possible to explain this apparent discrepancy between IR and SAXS measurements as a function of temperature by considering that SAXS intensity is derived from a coherent stacking of multilayers whereas the polarization of IR bands results from orientation of individual alkyl tails. Thus stacking faults would cause a loss of SAXS intensity but not a reduction in polarized IR band intensity.

The high-temperature behavior of preformed polymer monolayers containing backbone spacer groups is in marked contrast to that observed[9] for fatty acid molecules where irreversible degradation was observed due to dissociation of the polar head groups at elevated temperatures. For such an increased thermal stability the incorporation of spacer groups play an important role. In conventional polymerized multilayers packing problems limit the thermal stability severely.[22,30] Our studies exemplify the stabilization role of flexible polymer backbones in maintaining the reversibility of side chain orientation and order.

Conclusion

Polarized IR studies of a series of copolymers containing a varying concentration of hydrophilic main chain spacers have revealed that there is a higher degree of side chain orientation (see Figure 9) when the main chain spacer is the longest (see Figure 1). This is due to the increased flexibility of the polymer backbone which allows more efficient organization of the alkyl side chains so that their axes are normal to the substrate surface. This enhanced flexibility is also believed to be the origin of the significant stability observed at high temperatures.

The molecular picture that results is one in which the side chains are oriented normal to the surface linked together by flexible main chain spacer groups. At elevated temperatures the alkyl tails disorder but they remain "tied" together by the amorphous polymer backbone which allows the alkyl tails to reorient when the temperature is reduced.

Acknowledgment. J. Rabolt acknowledges partial support of this work by the Office of Naval Research Chemistry Division.

Registry No. $(H_3C(CH_2)_{17})_2NCO(CH_2)_2CO_2(CH_2)_2OCOC(CH_3){=}CH_2$ (homopolymer), 105473-58-3; $((H_3C(CH_2)_{17})_2NCO(CH_2)_2CO_2(CH_2)_2OCOC(CH_3){=}CH_2)(HO(CH_2)_2OCOCH{=}CH_2)$ (copolymer), 105473-59-4.

References and Notes

(1) Roberts, G. G.; Vincett, P. S.; Barlow, W. A. *Phys. Technol.* **1981**, *12*, 69.
(2) Ginnai, T. M. *Ind. Eng. Chem. Prod. Res.* **1985**, *24*, 188.
(3) Kuhn, H.; Möbius, D.; Bücher, H. *Physical Methods of Chemistry*; Weissberger, A.; Rossiter, B., Eds.; Wiley: New York, 1972; Vol. 1, p 577.
(4) Chollet, P.; Messier, J.; Rosilio, C. *J. Chem. Phys.* **1976**, *64*, 1042. Chollet, P. *Thin Solid Films* **1978**, *52*, 343.
(5) Ohnishi, T.; Ishitani, A.; Ishida, H.; Yamamoto, N.; Tsubomura, H. *J. Phys. Chem.* **1978**, *82*, 1989.
(6) Allara, D. L.; Swalen, J. D. *J. Phys. Chem.* **1982**, *86*, 2700.
(7) Rabolt, J. F.; Burns, F. C.; Schlotter, N. E.; Swalen, J. D. *J. Chem. Phys.* **1983**, *78*, 946.
(8) Blodgett, K. B. *Phys. Rev.* **1939**, *55*, 391. Stenhagen, E. *Trans. Faraday Soc.* **1938**, *34*, 1328. Gaines, G. L.; Roberts, R. W. *Nature (London)* **1963**, *197*, 787.
(9) Naselli, C.; Rabolt, J. F.; Swalen, J. D. *J. Chem. Phys.* **1985**, *82*, 2136. Naselli, C.; Rabe, J. P.; Rabolt, J. F.; Swalen, J. P. *Thin Solid Films* **1985**, *134*, 173.
(10) Cemel, A.; Fort, T.; Lando, J. B. *J. Polym. Sci., Polym. Chem. Ed.* **1972**, *10*, 2061.
(11) Fukuda, K.; Shibasaki, Y.; Nakahura, H. Proceedings 6th Internation Congress on Surface-Active Substrates; Zürich, 1972; Vol. 2, p 273.
(12) Ackermann, R.; Naegele, D.; Ringsdorf, H. *Makromol. Chem.* **1974**, *175*, 699.
(13) Tieke, B.; Graf, H. J.; Wegner, G.; Naegele, D.; Ringsdorf, H.; Bannerjie, A.; Day, D.; Lando, J. B. *Colloid Polym. Sci.* **1977**, *255*, 521.
(14) Barraud, A. *Thin Solid Films* **1983**, *99*, 317.
(15) Sarkar, M.; Lando, J. B. *Thin Solid Films* **1983**, *99*, 119.
(16) Laschewsky, A.; Ringsdorf, H.; Schmidt, G. *Thin Solid Films* **1985**, *134*, 153.
(17) Elbert, R.; Laschewsky, A.; Ringsdorf, H. *J. Am. Chem. Soc.* **1985**, *107*, 4134.
(18) Tredgold, R. H.; Winter, C. S. *J. Phys. D* **1982**, *15*, L55. Jones, R.; Winter, C. S.; Tredgold, R. H.; Hodge, P.; Hoorfar, A. *Polymer* **1987**, *28*, 1619.
(19) Mumby, S. J.; Swalen, J. D.; Rabolt, J. F. *Macromolecules* **1986**, *19*, 1054.
(20) Laschewsky, A.; Ringsdorf, H.; Schmidt, G.; Schneider, J. *J. Am. Chem. Soc.* **1987**, *109*, 788.
(21) Ringsdorf, H.; Schmidt, G.; Schneider, J. *Thin Solid Films* **1987**, *152*, 207. Biddle, M. B.; Lando, J. B.; Ringsdorf, H.; Schmidt, G.; Schneider, J. *Colloid Polym. Sci.*, submitted for publication.
(22) Laschewsky, A.; Ringsdorf, H.; Schmidt, G. *Polym. Prepr. (Am. Chem. Soc., Div. Polym. Chem.)* **1987**, *28*(1), 1315. Laschewsky, A.; Ringsdorf, H.; Schmidt, G. *Polymer* **1988**, *29*, 448.
(23) Gaines, G. L. *Insoluble Monolayers at Liquid-Gas Interfaces*; Wiley: New York, 1966.
(24) Frey, W.; Schneider, J.; Ringsdorf, H.; Sackmann, E. *Macromolecules* **1987**, *20*, 1312.
(25) Greenler, R. G. *J. Chem. Phys.* **1966**, *44*, 310.
(26) Rabolt, J. F.; Jurich, M.; Swalen, J. D. *Appl. Spectrosc.* **1985**, *39*, 269.
(27) Schlotter, N. E.; Rabolt, J. F. *Appl. Spectrosc.* **1985**, *39*, 994.
(28) Miyazawa, T.; Fukushima, K.; Ideguchi, Y. *J. Chem. Phys.* **1962**, *37*, 2764.
(29) Schneider, J.; Ringsdorf, H.; Schmidt, G., unpublished results.
(30) Rabe, J. P.; Rabolt, J. F.; Brown, C. A.; Swalen, J. P. *J. Chem. Phys.* **1986**, *84*, 4096.